



Fitting litter decomposition datasets to mathematical curves: Towards a generalised exponential approach

Pere Rovira ^{a,*}, Ricard Rovira ^b

^a Centre Tecnològic Forestal de Catalunya (CTFC), Ctra Sant Llorenç de Morunys km 2, 25280 Solsona, Catalunya, Spain

^b IES Matadepera, Avda Mas Sot 4-10, 08230 Matadepera, Catalunya, Spain

ARTICLE INFO

Article history:

Received 4 November 2008

Received in revised form 9 November 2009

Accepted 27 November 2009

Available online 20 January 2010

Keywords:

Litter

Decomposition

Kinetics

Mathematical models

Exponential models

ABSTRACT

The use of exponential functions to fit decomposition datasets is common in scientific literature. Olson's exponential equation ($X_t = X_0 e^{-kt}$) is widely used, but when strong curvatures are observed, the decomposing organic matter is commonly split into two compartments (*Labile* and *Recalcitrant*), thus obtaining double-exponential equations that often provide a good fit. Nevertheless, to correlate the so-calculated pools with quantifiable organic fractions is often very difficult, if not impossible. This suggests that even though these equations fit the experimental data well, they do not necessarily reflect what really happens in the decomposition process. The alternative is to apply models in which the organic matter, instead of being split into labile and recalcitrant compartments, is taken as a single pool whose decomposition rate is not constant.

Here we propose a general approach, which considers a single organic compartment. While the original exponential function that fits the basic equation is $dX/dt = -kX$, here we substitute the constant k by a function, $f(t)$, i.e. the decomposition rate is assumed to vary with time. Whatever function we choose, the remaining organic matter at time t is:

$$X_t = X_0 \cdot e^{-\int_0^t f(t) dt}$$

and thus the problem being addressed is how to integrate the function that describes the change in the decomposition rate. In this paper we study four possible dynamics for such a change: (1) an exponential decay, (2) a wave-form change, simulating seasonal rhythms, (3) a sigmoidal increase or decrease, and (4) a rational-type dynamics, involving an increase in the initial phase, followed by a gradual decrease. For each one, the integrated form is calculated, and some practical examples are given. Given its flexibility, our approach allows a good fit for a wide number of datasets, including those that well fit a single-exponential function, the classic Olson's function strictly being a specific case of the general equation we suggest.

© 2009 Elsevier B.V. All rights reserved.

1. Introduction

Litter decomposition has been one of the most popular topics in ecological research for many years. Organic matter decomposition enables a massive recycling of chemical elements on the scale of ecosystems and the whole biosphere (Berg and Laskowski, 2006). It represents a main step in the global carbon cycle in terrestrial ecosystems and, thanks to the availability of study methods, and more specifically to the widely known litter-bag methods, it is easy to access sets of field data.

Computer models (Century, SOMM, Candy, etc), which try to simulate the processes that provoke the overall decomposition process, have been applied to study litter decomposition (Zhang et al., 2008). However, most

researchers have looked for single, direct mathematical descriptions of the overall phenomenon, by fitting decay functions to remaining mass values. A decay function, simpler than a computer model, can be advantageous if the main aim of the researcher is to summarise the main features of the studied decomposition datasets to allow for an easy and direct comparison between them. Fitting decomposition datasets to a theoretical equation may be of great value if the equation has been designed to reflect the mechanisms that result in the overall process.

Not surprisingly, a great number of equations have been proposed, from the first proposal of Jenny et al. (1949) to recent approaches (Yang and Janssen, 2000). Despite a considerable number of years since its publication, the approach of Jenny et al. (1949), further developed in detail by Olson (1963), is still the most popular one. In this approach, litter decomposition follows a single-exponential dynamics, in the form

$$X_t = X_0 e^{-kt} \quad (1)$$

* Corresponding author.

E-mail address: pere.rovira@ctfc.cat (P. Rovira).

where X_t is the amount of litter at time t , X_0 the initial amount, and k the decomposition rate. The basic assumption is that k is constant. This simple equation has been applied extensively. Nevertheless, in litter decomposition studies, dynamics with a strong curvature that cannot fit a single-exponential equation, are often obtained. This is explained by the changes in the decomposing litter: some components are degraded first (carbohydrates, hemicelluloses, water-soluble compounds, etc), while others remain much longer (waxes, lignin, suberins, etc.) (Minderman, 1968; Berg et al., 1982; Rovira and Vallejo, 2000). As the former disappear and the latter accumulate, k decreases. Quadratic or power models have been used in these cases (reviewed by Wieder and Lang, 1982) but, most commonly, the phenomenon has been explained by assuming that the whole litter at zero time (X_0 , in Eq. (1)) is split into a number of compartments ($i = 1, 2, \dots, n$), each having its own decomposition rate k_i . This is translated into a multiple-exponential equation:

$$X_t = \sum_{i=1}^n X_{i0} e^{-k_i t} \quad (2)$$

In practice, up to three compartments have been considered (e.g., Adair et al., 2008). However the most usual approach is to set $n = 2$, i.e., the whole litter is assumed to be split into a 'labile' and a 'recalcitrant' pool, differing in their decomposition rates:

$$X_t = a e^{-k_1 t} + b e^{-k_2 t} \quad (3)$$

where a is the initial amount of the labile pool and k_1 its decomposition rate, and b the initial amount of the recalcitrant pool and k_2 its decomposition rate. By definition, $k_1 > k_2$. It is usually assumed that the sum $a + b$ is equal to the whole initial litter. If we work with percentages, then $a + b = 100$, and therefore $b = 100 - a$. I.e., a three-parameter equation is finally obtained. This approach usually gives better fits than Olson's single-exponential equation, and is widely used (e.g., Lousier and Parkinson, 1976; Gillon et al., 1993; Rovira and Vallejo, 1997, 2000). Even in studies not directly linked to the application of an exponential dynamics (e.g. Couëteux et al., 2001), the splitting of litter into a labile and a recalcitrant pool is assumed. These standard exponential models can be refined if correctors for the several k are applied, to account for climatic variability (e.g., Adair et al., 2008).

These compartments can sometimes be identified with defined components of the decomposing litter, such as cellulose or lignin (Adair et al., 2008), but not always (Dendooven et al., 1997; Rovira and Vallejo, 2000; Vaieretti et al., 2005). Strictly, Eqs. (2) and (3) involve two basic assumptions which are known to be wrong: (i) that the several compartments decompose independently, without any interaction between them, and (ii) that the quality of the several compartments does not appreciably change with time, since their decomposition rates are constant. Whatever the criteria we apply to separate a labile from a recalcitrant pool (acid hydrolysis, thermogravimetry, etc), we will find that both pools do not behave independently (e.g., Rovira and Vallejo, 2002), and that they suffer biochemical changes with time (e.g., Rovira et al., 2008). Highly recalcitrant polymers release less recalcitrant monomers to the labile compartment, whereas the labile compartment also releases organic matter to the recalcitrant one when labile compounds evolve to poorly biodegradable compounds, for instance through the generation of refractory polymers between lignin or polyphenols and N (Nömmik and Vahtras, 1982; Kelley and Stevenson, 1996; Berg and Laskowski, 2006). Even though a double-exponential equation can be very useful to fit the data, it does not necessarily reflect what really occurs during decomposition.

Carpenter (1981) overcomes this drawback by considering the decomposing organic matter as a continuum of pools varying in their quality, from 0 (the most refractory) to 1 (the most labile). These

pools are not meant to be independent, but related to each other: there is a generation of both labile and recalcitrant organic matter during the decomposition process, following well defined laws. The concept of a continuum of qualities within the whole decomposing organic matter was also developed in detail by Bosatta and Ågren (1985, 1991). In spite of the great theoretical interest—and even beauty—of these approaches, they have not been widely applied, owing probably to the mathematical complexity of the resulting equations. The most recent development in line with this approach is the K-Model (Feng, 2009a,b,c), which also reaches a considerable mathematical complexity.

The alternative—and simpler—approach is to consider a single organic compartment, whose decomposition rate changes with time. This is the strategy adopted in this paper.

Before our study, there have been several attempts in this direction: Carpenter (1982), Ezcurra and Becerra (1987), Montaña et al. (1988) and Yang and Janssen (2000), have suggested or applied flexible single-compartment models. A feature of these models is that in most of them k is assumed to decrease with time. In a natural environment, this does not always happen: fluctuations in k may occur, due either to seasonal cycles or to the changing physical position of the litter within the soil profile. While the first organic layers (O_L) are often subjected to strong drying events, the deep organic layers have a more constant water regime: subsequently, the decomposition rate of a given cohort of litter can increase in these horizons. It is also possible to observe an initial lag phase in the decomposition if a period of microbial colonisation in the surface of the organic debris is needed (Wolters and Schaefer, 1993).

Hereafter we present an alternative approach to the analysis of decomposition kinetics, more flexible than those mentioned above: not a single equation, but a global conceptual solution, which, in practice, can take different forms depending on the dataset being studied. The aims of this paper are as follows:

1. To introduce a generic mathematical approach to obtain curves to fit decomposition datasets.
2. To develop several specific examples of this approach: each one of these is representative of situations that can be found in nature.
3. To apply these examples to real decomposition datasets, to show how our approach allows us to obtain not only good fitting curves, but also relevant information concerning the dynamics of the decomposition process.

2. Materials and methods

2.1. Mathematical description

Henceforth we will call r the instantaneous decomposition rate; only when r is constant will we use the term k .

To understand our approach we must refer back to the original concept of Jenny et al. (1949), as developed by Olson (1963). In the approach of Jenny and Olson, r is assumed to be constant (i.e., k). Given in differential equation terms:

$$\frac{dX}{X} = -k dt \quad (4)$$

where X is the amount of litter in a given moment, k the instantaneous decomposition rate, and t the time. We integrate Eq. (4), to obtain the remaining litter at time t (i.e., X_t):

$$\ln(X_t) = -kt + \ln(X_0) \quad (5)$$

where X_0 is the amount of litter at time zero. Taking antilogarithms, we obtain the classical single-exponential model, widely known and applied:

$$X = X_0 e^{-kt} \quad (6)$$

If the decomposition rate r is not constant, but changes in a way that can be mathematically described as a function of time, $f(t)$, then Eq. (4) can be rewritten in a more generic form:

$$\frac{dX}{X} = f(t)dt \tag{7}$$

We integrate Eq. (7), to obtain a new generic equation, which fits the experimental data when the decomposition rate cannot be assumed as constant:

$$X_t = X_0 e^{-\left(\int_0^t f(t)dt\right)} \tag{8}$$

Thus, the whole problem of fitting a decomposition dataset to a theoretical curve is reduced to: first, detecting a function $f(t)$ that describes the behaviour of r , and, second, integrating $f(t)$. The Olson's model is merely a specific example of Eq. (7), in which $f(t) = k$ (constant). A priori, $f(t)$ could be any function. However, $f(t)$ must not only be correct in mathematical terms, but also logical in biological terms, which limits the options. For instance, decomposition implies, strictly speaking, a loss of organic matter: therefore, $f(t)$ can never be negative.

Henceforth, several possible changes in r will be examined. Since all of them match situations that can be seen in nature, they are expected to give integrated equations capable of fitting—and, at least partly, explaining—several dynamics sometimes found in decomposition experiments. In this section we only show the initial functions and their integrated forms; a description of how we obtained the functions is detailed in Appendix A.

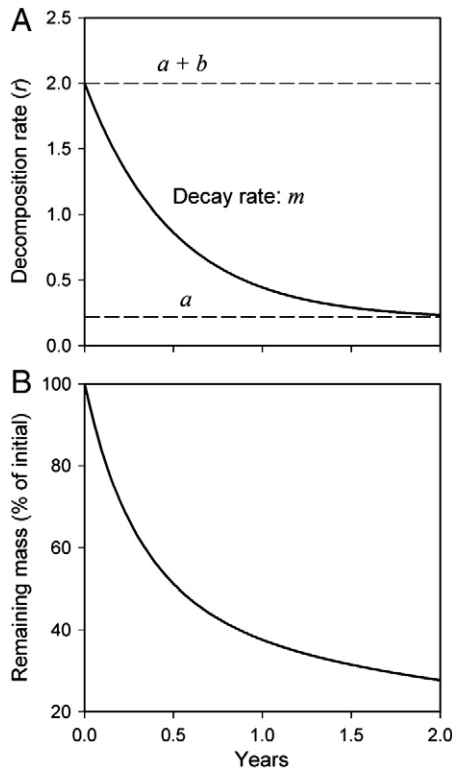


Fig. 1. Main features of the composite-exponential function for r . A: Decomposition rate. B: Remaining mass, resulting from the changing decomposition rate. The initial decomposition rate ($a + b$) changes to the final rate (a) following an exponential curve, m being the decay rate. Usually a , b and m are positive: which means that the decomposition rate will decrease with time. In the example given, $a = 0.2$, $b = 1.8$, $m = 2$.

Case 1. Exponential decrease of the decomposition rate (Fig. 1).

The decomposition rate r decreases from an initial value ($a + b$, at $t = 0$) to a final value (a , at $t = \infty$). The change follows an exponential curve. That is,

$$f(t) = a + be^{-mt} \tag{9}$$

where m is the exponential rate of decay of b . Since both a , b and m are instantaneous rates, their units are the same: time^{-1} . We must note that the change is not necessarily a decrease: if either b or m is negative, the decomposition rate will increase. In contrast, a must be always ≥ 0 ; if a is negative, then the decomposition rate can eventually be negative, and this is not possible in a decomposition process.

We integrate Eq. (9) relative to t , to obtain:

$$\int_0^t f(t)dt = at - \frac{b}{m}(e^{-mt} - 1) \tag{10}$$

To obtain the decay curve, we must replace Eq. (10) in Eq. (8).

Case 2. Wave-form dynamics of the decomposition rate (Fig. 2).

Such a dynamics is to be expected in ecosystems subjected to strong seasonal changes, resulting in rhythmic fluctuations in r . If the decomposing litter is sampled at intervals small enough to reflect these changes (e.g. 1–3 months), it is possible to detect rhythms in the decomposition process, which usually result in datasets hard to fit with the usual exponential curves.

The seasonal changes in r can be approached by a trigonometric function:

$$f(t) = m + a \sin\left(\frac{2\pi}{b}t + c\right) \tag{11}$$

where m is the mean value of r , a is the amplitude of the change (i.e., the possible values for r are between $m + a$ and $m - a$), b is the amplitude of the period, and c is the angular shift in the cycle (i.e., the decomposition does not necessarily start when the decomposition rate is $r = m$). Fig. 2 illustrates the meaning of all these parameters. Since a and m are possible values for r , then both have the same units: time^{-1} . In contrast, b represents time lags, and its units are time units (days, months, etc.).

An important constraint is $a \leq m$. If $a > m$, the decomposition rate r would be negative at some stage, which biologically speaking is impossible. The period (b) can be forced to 1 year, and thus the function becomes simplified, with only 3 parameters instead of 4.

By integrating Eq. (11), we obtain

$$\int_0^t f(t)dt = mt - \frac{ab}{2\pi} \left[\cos\left(\frac{2\pi}{b}t + c\right) - \cos c \right] \tag{12}$$

To obtain the decay curve, we must replace Eq. (12) in Eq. (8).

Case 3. Sigmoidal change of the decomposition rate (Fig. 3).

The change in r can take a sigmoidal-type shape when there is a change in the conditions under which the decomposition takes place. This shift in r can be negative: in waterlogged soils, for instance, r may drop when, after a period in a well-oxygenated L horizon, litter reaches an F or H horizon with low oxygen availability. The shift can be also positive: the initial r may be low, due to a constraint that may reduce even further. For instance, where there is a lack of microbial biomass: as soon as the litter surface has been massively colonised by microflora, an activation of the decomposition process is likely to happen.

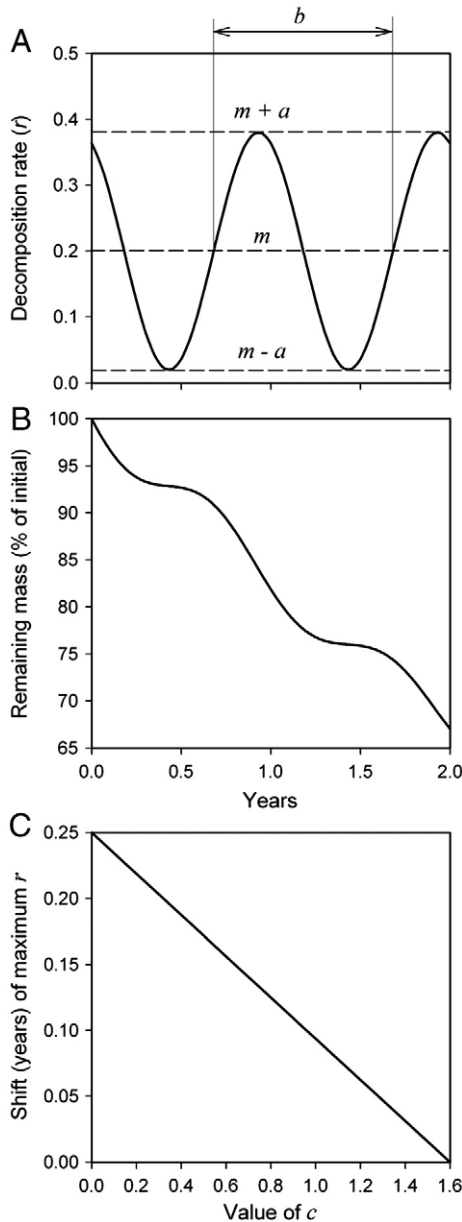


Fig. 2. Main features of the sinusoidal function for r . A: Decomposition rate. The decomposition rate changes rhythmically: m is the mean value of r , a is the amplitude, b the length of a cycle, and c the angular shift between the start of the experiment and the start of a cycle. For an annual seasonal cycle, b should be 1 year. In this example, $a=0.18$, $b=1$, $c=2$ and $m=0.2$. B: Remaining mass, resulting from the changing decomposition rate. C: relationship between the c value and the shift (in years) in the position of the maximum r value, relative to the start of the decomposition.

Many curves described in mathematical literature could be used here. We can suggest, because of its simplicity (four parameters only):

$$f(t) = \frac{a}{1 + e^{\frac{t-t_0}{b}}} + c \quad (13)$$

in which b (adimensional) gives the shape of the function, because if $b < 0$, then r decreases with time, whereas if $b > 0$ then r increases. The lower the absolute value of b , the faster the increase or decrease in r . As for a and c , both are time^{-1} : the sum $a + c$ gives the uppermost value for r , and c the lowermost. The moment in which the change occurs is given by t_0 , which gives the time at which r is exactly at the

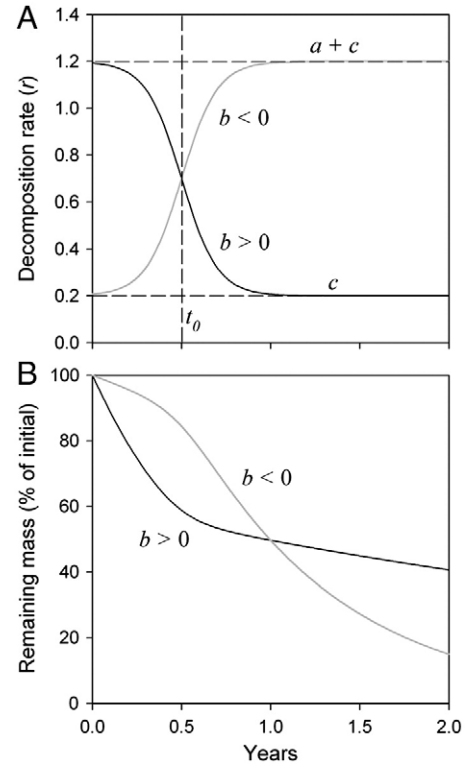


Fig. 3. Main features of the sigmoidal function for r . A: Decomposition rate. B: Remaining mass, as resulting from the changing decomposition rate. The maximum value for r is given by $a + c$, while the minimum is given by c . The parameter b gives the speed at which the change from the initial to the final value will occur: the smaller the absolute value of b , the faster the change. The sign of b determines the sense of the change: if $b > 0$, the decomposition rate increases (grey line), while if $b < 0$ the decomposition rate decreases (black line). The parameter t_0 gives the middle point of the change in r . In this example, $a = 1$, $b = 0.1$ or -0.1 , $c = 0.2$ and $t_0 = 0.5$.

mean point between the lowermost (c) and the uppermost ($a + c$) value. The meaning of these parameters is shown in Fig. 3.

We integrate Eq. (13) relative to t , thus obtaining

$$\int_0^t f(t) dt = ct + a \left[t - b \ln \frac{1 + e^{-(t_0-t)/b}}{1 + e^{-t_0/b}} \right] \quad (14)$$

To obtain the decay curve, we must replace Eq. (14) in Eq. (8).

Case 4. Rational-type change in the decomposition rate (Fig. 4).

The decomposition rate may show a strong initial increase, and a decrease thereafter (for instance, Wolters and Schaefer, 1993). There can be several reasons for such a pattern: for instance, an initial period of microbial colonisation may be needed before the decomposition process starts. This reason has already been mentioned to explain a sigmoidal-type increase for r ; but the main difference is that, whereas in the sigmoidal dynamics the decomposition rate r is assumed to remain constant after the period of increase, in the rational-type dynamics r is assumed to decrease gradually, after reaching its maximum value.

Among many other possibilities, we suggest the following equation for the rational-type change:

$$f(t) = c + \left(\frac{at}{t^2 + b} \right)^d \quad (15)$$

Fig. 4 illustrates the meaning of the various parameters, which in this equation are less obvious than in Cases 1–3. In this equation, c is the lowermost value for r , and is found at time $t = 0$ and at time $t = \infty$.

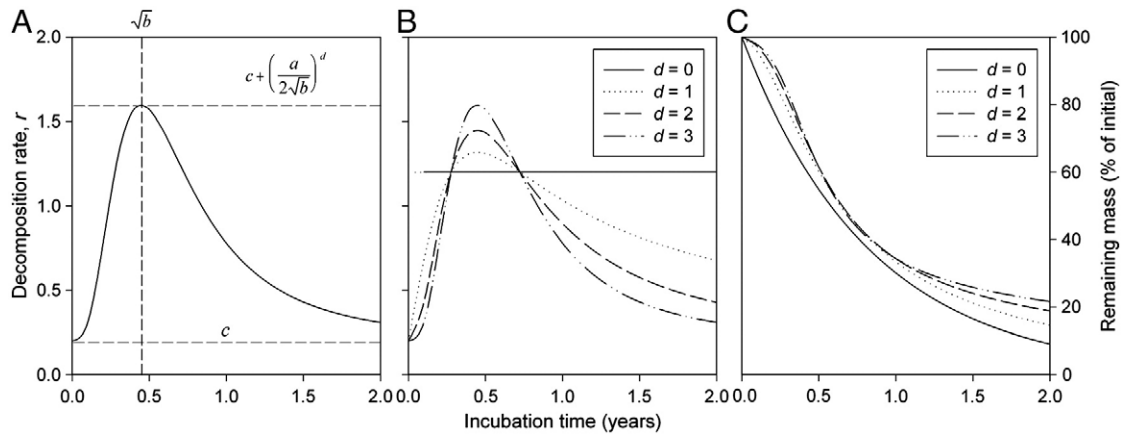


Fig. 4. Main features of the rational function for r . In these examples, $a = 1$, $b = 0.2$ and $c = 0.2$. A: Decomposition rate. In this example, $d = 3$. The initial and final values for r are given by the constant term, c , while the square root of b gives the time at which r reaches its maximum. B: Evolution of the decomposition rate for contrasting d values. As d increases, the change in the decomposition rate (increase and further decrease) concentrates around the maximum value. C: Remaining mass, resulting from the changing decomposition rate, for several d values. The 'S' shape becomes stronger as d increases.

The parameter b (actually, its square root) gives the time at which the decomposition rate reaches its uppermost value; this uppermost value is given by

$$r_{max} = c + \left(\frac{a}{2\sqrt{b}}\right)^d \tag{16}$$

The exponent d (non-dimensional) determines the speed of increase and further decrease in the decomposition rate, r . When $d = 0$, r is a constant ($r = c$); as d increases, the change in r becomes more concentrated around the uppermost point.

There is no single solution integral to Eq. (15). The solution is different for each value of d . For $d = 1$, the solution is rather immediate:

$$\int_0^t f(t)dt = ct + \frac{a}{2} \ln\left(\frac{x^2 + b}{b}\right) \tag{17}$$

For $d > 1$, the general solution is:

$$\int_0^t f(t)dt = ct + \frac{a^d}{\sqrt{b}^{d-1}} \left\{ \frac{1}{2-2d} \left[\left(\frac{z}{z^2 + 1}\right)^{d-1} \right]_0^{t/\sqrt{b}} + \frac{1}{2} \int_0^{t/\sqrt{b}} \frac{z^{d-2}}{(z^2 + 1)^{d-1}} dz \right\} \tag{18}$$

which is obtained through a change of variable: $t = z\sqrt{b}$. For $d = 2$, Eq. (18) becomes:

$$\int_0^t f(t)dt = ct + \frac{a^2}{2\sqrt{b}} \arctan\frac{t}{\sqrt{b}} - \frac{a^2 t}{2(t^2 + b)} \tag{19}$$

whereas for $d = 3$, becomes:

$$\int_0^t f(t)dt = ct + \frac{a^3}{4b} \frac{t^4}{(t^2 + b)^2} \tag{20}$$

To obtain the decay curve, we must replace Eq. (17), (19) or (20) in Eq. (8).

In practice, we always apply Eq. (20), i.e., we assume $d = 3$. The reason is obvious from Fig. 4C: the 'S' shape is clear only when $d = 3$. When $d < 3$ the calculated decay curves are very similar to a typical composite-exponential curve, which means that the initial peak in microbial activity is barely reflected in the integral curve during the

first decomposition stages. In this case, the choice of a rational equation for r , more complex than the composite-exponential one, would not be justified.

2.2. Datasets used in the study

To evaluate the extent to which our approach satisfies the most common situations arising in litter decomposition studies, we have taken data from previously published datasets. The main criterion for our selection was their intrinsic quality, i.e., the clearness and consistency of the observed trends, with data dispersion as low as possible.

1. Dataset A. This includes three experiments of litter decomposition carried out at Jädraås (Sweden): Scots pine (*Pinus sylvestris*) needles, incubated for >5 years; birch (*Betula pubescens*) leaves, incubated for 4 years; and cowberry (*Vaccinium vitis-idaea*) leaves, incubated for 2 years. The numerical data have been taken from Berg et al. (1984).
2. Dataset B. This includes three experiments of litter decomposition carried out at Blackhawk Island (Wisconsin, USA) for 2 years: white pine (*Pinus strobus*), white oak (*Quercus alba*) and red oak (*Quercus borealis*); original data taken from Berg et al. (1984).
3. Dataset C. This dataset includes litter from four species: aspen (*Populus tremula*), Scots pine (*P. sylvestris*), silver birch (*B. pubescens*), and stone pine (*Pinus pinea*). Two sets of litter (aspen and scots pine) were incubated both as green and brown needles. All litter were submitted to field decomposition experiments in Jädraås (Sweden) and Monte Taburno (Italy); original data summarised in Berg et al. (2003).
4. Dataset D. Data taken from Rahman Barbhuiya et al. (2008). Litter-bag experiments in the Namdapha National Park, northeast India. Due to the tropical conditions, decomposition was much faster than in the previous datasets, and the majority, if not all of the incubated litter, was lost in a single year. The dataset includes ten different species.
5. Dataset E. Data taken from Li et al. (2007). Litter decomposition studies carried out in Fusong (NW China). The dataset includes nine different tree species, incubated in the field for almost 3 years.

For some datasets it was not possible to obtain the original numerical data. In these cases, the amounts of remaining litter were obtained from the original paper in PDF form, by translating the document into a Corel Draw v.11 graph, and positioning the points accurately using the tools of this software.

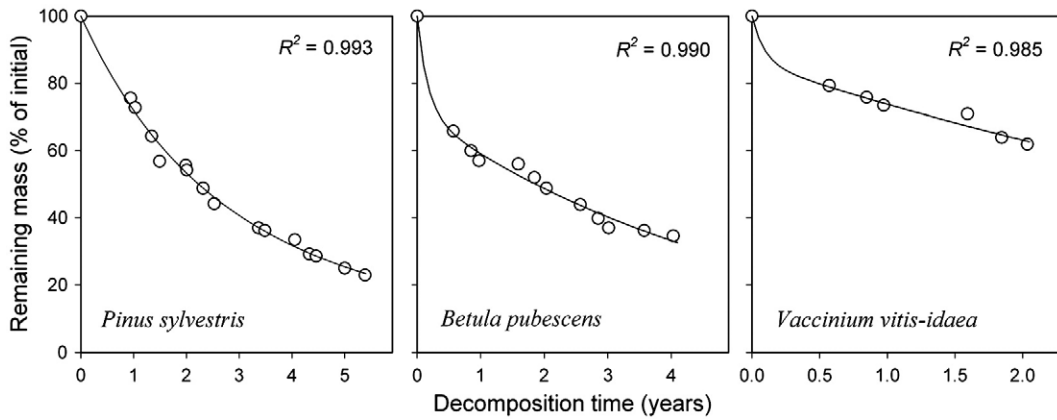


Fig. 5. Results obtained for dataset A. Experimental data have been fitted to both a double-exponential (Eq. (3)) and to a composite-exponential model (Eq. (10), placed in Eq. (8)). The curves obtained for both models were virtually identical, and therefore only the latter has been drawn. The parameters of the obtained curves are given in Table 1. The R^2 values were the same for both models.

2.3. Statistical analysis

In order to select an equation for curve fitting (either composite-exponential, sinusoidal, sigmoidal, or rational), we compared the datasets with the plots of remaining weight as they result from the proposed equations (i.e., Figs. 1B, 2B, 3B and 4C); using visual comparison it is easy to detect which equation is the most appropriate for each dataset.

Curve fitting was carried out with the NCSST statistical package, which uses the iterative Marquardt–Levenberg algorithm to obtain the best values for all parameters. Since the success of this algorithm (i.e., the obtaining of convergent values for the curve parameters) depends on the initial values given to these parameters, we previously approached credible values for each of them using a conventional computer spreadsheet.

In addition to the fitted equation (composite-exponential, sinusoidal, sigmoidal, and rational) we also fitted all datasets to the classic Olson's model, in order to show how the equations we suggest improve the fit. There is indeed an improvement, but at the price of an increase in the number of parameters involved. As the estimation of each parameter contains a margin of error, more uncertainty may have been added to the model, in spite of the improvement in fit. To account for this problem, the Akaike's Information Criterion (AIC) is often applied (see Anderson, 2008, for a detailed description). AIC is a measure of the deviance of any proposed model, relative to the (unknown) 'true' model. It is usually written as

$$AIC = -2 \log L[(\theta|x)] + 2K \tag{21}$$

where $L[(\theta|x)]$ is the maximized likelihood of the model, given the estimated parameters and the available data, and K the number of parameters involved in the model. Usually, the best-fitting values for the

Table 1
Dataset A (Berg et al., 1984). Parameters of the best-fitting double-exponential curves obtained (Eq. (3)), and those of the best-fitting composite-exponential curves obtained (Eq. (10), placed in Eq. (8)). The degree of fit (R^2) was identical for both (Fig. 5).

Species	Double-exponential			Composite-exponential		
	<i>a</i>	<i>b</i>	<i>c</i>	<i>a</i>	<i>b</i>	<i>m</i>
<i>Pinus sylvestris</i>	46.49	0.1573	0.5074	0.0467	0.2995	0.1157
<i>Betula pubescens</i>	71.39	0.1912	5.7079	0.1913	1.7942	5.3327
<i>Vaccinium vitis-idaea</i>	86.61	0.1559	10.8597	0.1559	1.5336	10.6678

parameters are not obtained through likelihood procedures, but through least squares regression. In this case, $\log(L)$ may be rewritten as

$$\log(L) = -\frac{n}{2} \log(\hat{\sigma}^2) \tag{22}$$

where n is the sample size, and $\hat{\sigma}^2$ is the residual variance. Thus Eq. (21) becomes

$$AIC = n \log(\hat{\sigma}^2) + 2K \tag{23}$$

By applying Eq. (23) to a given model applied to a given dataset, a numerical value is obtained. This number increases with increasing either the residual variance, n , or K . Two models, applied to the same dataset, will give different AIC values. The model closest to the true (and unknown) model is the one having the lowest AIC number. This criterion, applied to our data, means that any of the proposed equations will be preferable to the classic Olson's model if $AIC_{OLSON} > AIC_{EQ}$, or, in other words, if $\Delta AIC < 0$, being $\Delta AIC = AIC_{EQ} - AIC_{OLSON}$.

It has been noted that AIC may perform poorly when the dataset is small (low n values), especially for high K values. A corrected version of the AIC (AIC_C) is then recommended:

$$AIC_C = AIC + \frac{2K(K+1)}{n-K-1} \tag{24}$$

We applied both AIC and AIC_C , because the comparison of ΔAIC and ΔAIC_C gives interesting information. If both are positive, then the

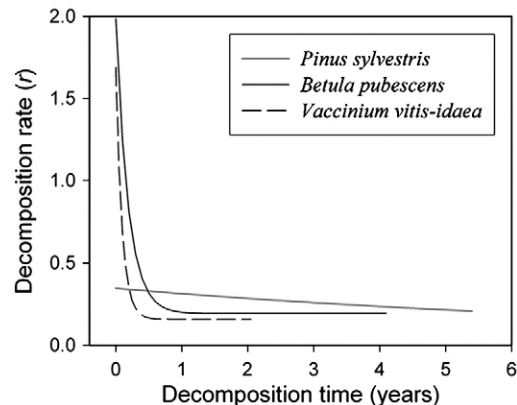


Fig. 6. Evolution of the decomposition rate in the experiments of dataset A, as obtained from the application of the composite-exponential model.

Table 2

Dataset B (Berg et al., 1984). Parameters of the best-fitting sinusoidal curves obtained (Eq. (12), placed in Eq. (8)). The obtained curves, together with the obtained R^2 values, are shown in Fig. 7.

Species	<i>m</i>	<i>a</i>	<i>b</i>	<i>c</i>
<i>Pinus strobus</i>	0.4353	0.4353	1.2737	3.8376
<i>Quercus alba</i>	0.5146	0.5146	1.0133	3.0049
<i>Quercus borealis</i>	0.4438	0.4018	1.3234	4.2358
<i>Quercus borealis</i> ^a	0.4377	0.4377	1.3145	4.1762

^a Improved model, assuming $X_0 < 100$ (see text).

replacement of the classic Olson's model by any of the proposed equations is not justified, in spite of the (expected) increase in R^2 . If ΔAIC is negative but ΔAIC_C is positive, the result is doubtful: the proposed equation may be closer to the truth, but the dataset is too small to state it clearly. Finally, if both ΔAIC and ΔAIC_C are negative, the proposed equation is clearly better than Olson's model for the studied dataset.

The obtained R^2 values for Olson's equation are given in Appendix A (Table A1), together with the R^2 values obtained with the equation we apply in each case, and the increases in both AIC and AIC_C values, when passing from Olson's model to the proposed equation.

3. Results

3.1. Dataset A (Berg et al., 1984)

The decomposition experiments of this dataset follow exponential-type decay (Fig. 5). The data can be fitted easily with a double-exponential model (Eq. (3)), but an equally good fit is achieved assuming an exponential decrease of the decomposition rate (Eq. (10)) (Table 1). Thus the latter can be seen as an alternative to the former, since the number of parameters to obtain it is the same (3, in both cases). The curves obtained from both equations are virtually identical (same R^2 values) and, therefore, only one graph has been drawn in Fig. 5 for each tree species.

The two models, however, explain the experimental data in a contrasting way: the double-exponential equation, on one hand, as the result of the persistence of a resistant pool against the rapid loss of a labile one; and the composite-exponential equation, on the other hand, as the result of a drop in the overall decomposition rate, without assuming any splitting of the decomposing litter into functional compartments.

Leaves of *Betula* and *Vaccinium* show initial decomposition rates ($a + b$) much higher than that of *Pinus*, but in *Pinus* the decomposition rate drops much more steadily: during most of the experiment its decomposition rate is higher than in the other litters, and this explains why, in the end, its decomposition is faster (Fig. 6). Actually, for *Pinus* the fit obtained by applying a single-exponential equation (Olson's

model) is quite high ($R^2 = 0.984$), and is only slightly improved when moving to a composite-exponential equation (Table A1).

3.2. Dataset B (Berg et al., 1984)

The results of the remaining litter in this dataset clearly show rhythms in the decomposition activity, and the periodicity of these rhythms (about 1 year) suggests a seasonal fluctuation in biological soil activity. From this apparent behaviour of r , we have assumed a sinusoidal-type function (Eq. (11)). The best-fitting parameters are given in Table 2; the plots resulting from the integrated equations, together with the overall R^2 values, are shown in Fig. 7.

The resulting fits are very close, particularly the first two ($R^2 = 0.997$ for *P. strobus*, $R^2 = 0.996$ for *Q. alba*) (Fig. 7). For *Q. borealis* the original fit was also good ($R^2 = 0.991$), and it was improved when considering X_0 as an additional parameter, i.e., by assuming that X_0 could be $\neq 100\%$. In this way we approached $X_0 = 98.3$, i.e., we assumed a loss of 2.7% of the initial litter at the very start of the field incubation, likely due to leaching. Thus, R^2 increases slightly, up to 0.993. This was not observed in the other litters, where whenever X_0 was added as a variable to fit the equation, the software always yielded $X_0 = 100$ as the best-fitting value.

The best-fitting values for the parameters (Table 2) show $m = a$. For *Q. borealis*, this occurs in the improved model, i.e., when $X_0 = 98.3$. Thus, at some stage the decomposition rate is $r = 0$, most likely in the winter. However, Eq. (11) implies that in the next cycle the decomposition rate recovers the previous maximum value. The good fit ($R^2 > 0.99$ in all cases) suggests that the seasonal cycle is enough to explain changes in r : it is not necessary to assume any additional processes that drive extra decreases in r . Our analysis on dataset B suggests that a detectable decrease in litter quality has not yet occurred even when, after two years, more than 50% of the initial litter has been lost. Thus the decomposition rate can be reasonably assumed as constant, only affected by a seasonal fluctuation. In agreement with this, the degree of fit reached by Olson's equation is also quite high (Table A1).

3.3. Dataset C (Berg et al., 2003)

All the experiments included in this dataset follow a relatively standard curvature, and therefore match a composite-exponential decomposition dynamics (Eq. (10)). The results of curve fitting are summarised in Fig. 8 and Table 3. In three cases, all in Monte Taburno, a (the lowermost limit for r) is zero. Nevertheless, this should occur at time $t = \infty$; thus the eventual accumulation of a true inert or almost inert residue should be null, in practice.

It is noteworthy that we have obtained negative values for b for the Lodgepole pine both at Jädraås and Monte Taburno, i.e., the decomposition rate increases with time.

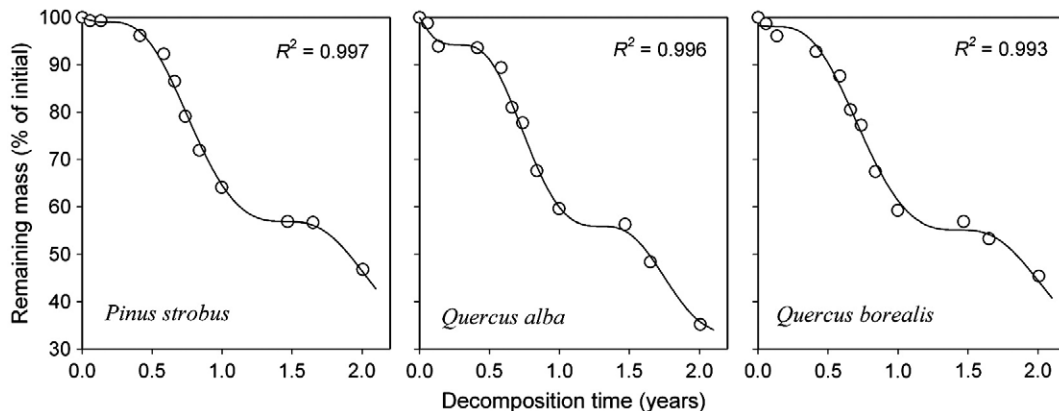


Fig. 7. Results obtained for dataset B. Experimental data have been fitted to a sinusoidal model (Eq. (12), placed in Eq. (8)). Parameters are given in Table 2.

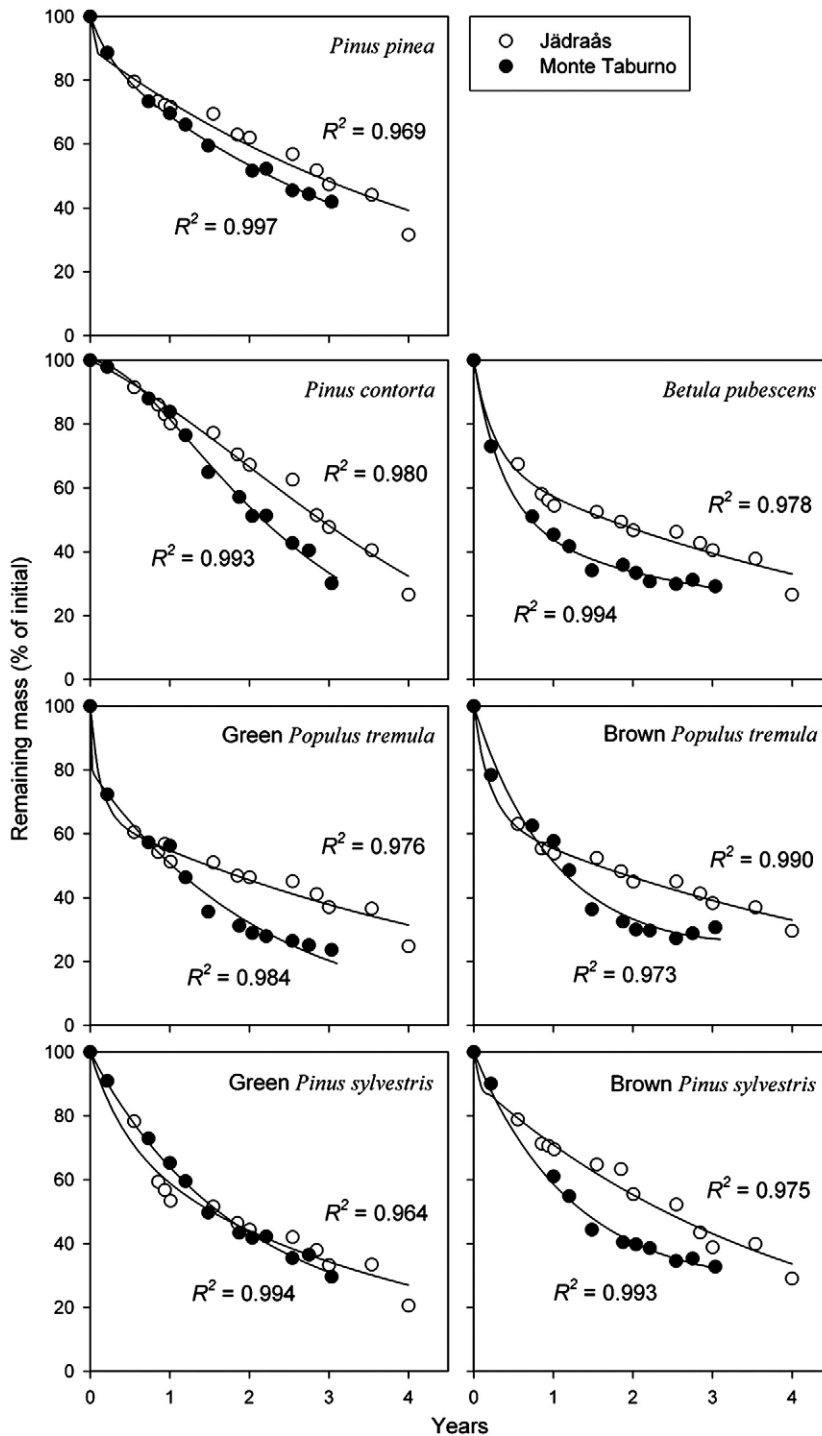


Fig. 8. Results obtained for dataset C. Experimental data have been fitted to a composite-exponential model (Eq. (10), placed in Eq. (8)). Parameters are given in Table 3.

Due to the homogeneity and extension of this dataset (14 litter-bag experiments in total, all described by the same equation), it is worth trying to detect a consistent relationship between the parameters of the curves obtained. We particularly focused on the relationship between the initial decomposition rate ($a + b$) and its decay rate (m). As shown in Fig. 9, both are directly related, i.e., the higher the initial decomposition rate, the faster its decay. This had also been observed for dataset A; here we see the phenomenon on a wider scale. The relationship is particularly clear for Jädraås datasets. When the decomposition rate shows just a slight decrease (i.e., in coniferous litters), the R^2 values attained with Olson's equation are close to those obtained with the composite-exponential equation, whereas for

broad-leaved litters, in contrast, the composite-exponential equation fits the datasets much better (Table A1).

In the original work, Berg et al. (2003) fitted the several datasets to the model

$$y = m \left(1 - e^{-\frac{kt}{m}} \right) \quad (25)$$

where y is the accumulated mass loss (in percent), t the time in days, m the (asymptotic) maximum accumulated mass loss, and k is the initial decomposition rate. Berg et al. (2003) gave only the m values for each experimental condition (litter type \times site); from them, however, and

Table 3

Dataset C (Berg et al., 2003). Parameters for the best-fitting composite-exponential curves obtained (Eq. (10), placed in Eq. (8)). The obtained curves are shown in Fig. 8, together with the obtained R^2 values.

Site	Species	<i>a</i>	<i>b</i>	<i>m</i>
Jädraås	Green <i>Populus tremula</i>	0.1853	2.8721	6.8950
	Brown <i>Populus tremula</i>	0.1709	1.8112	4.2484
	Green <i>Pinus sylvestris</i>	0.2383	0.5920	1.6572
	Brown <i>Pinus sylvestris</i>	0.2490	4.5302	48.1034
	<i>Pinus contorta</i>	3.1646	−3.0435	0.0274
	<i>Betula pubescens</i>	0.1787	1.2990	3.3095
	<i>Pinus pinea</i>	0.2076	5.1559	49.8298
Monte Taburno	Green <i>Populus tremula</i>	0.4581	28.1787	127.8485
	Brown <i>Populus tremula</i>	0.0000	0.8313	0.4613
	Green <i>Pinus sylvestris</i>	0.0000	0.4787	0.1407
	Brown <i>Pinus sylvestris</i>	0.0000	0.6400	0.3784
	<i>Pinus contorta</i>	0.5238	−0.5094	1.0214
	<i>Betula pubescens</i>	0.1389	1.4384	1.7207
	<i>Pinus pinea</i>	0.2488	0.4322	3.3146

from the data of mass loss, we have calculated the k values, and the R^2 values obtained when fitting Eq. (21) to the data (Table 4). Eq. (21) gave overall a good fit; the mean R^2 value is 0.958 ± 0.026 . Our approach gives overall a better fit, with a mean R^2 value of 0.976 ± 0.019 . Strictly speaking, Eq. (21) implies (when $m < 100\%$) that a fraction of the decomposing litter is indecomposable, which is difficult to accept. Actually Berg et al. (1996) stress that the term $[100 - m]$ must be meant not as a truly inert compartment, but as a fraction which decomposes very slowly. Our approach (Eq. (8)) lacks this conceptual problem because it does not assume the existence of any inert fraction, even though it needs one more parameter (3, instead of 2).

3.4. Dataset D (Rahman Barbhuiya et al., 2008)

The decomposition experiments of dataset D can be thoroughly explained by assuming a positive-sigmoidal increase of the decomposition rate r (Fig. 10). The best-fitting parameters obtained are provided in Table 5. The degree of the fit is excellent: R^2 values are always > 0.99 , much higher than those reached with the single-exponential equation (Table A1), and in spite of the increase in K (4 parameters are needed), the Akaike criterion clearly states that a sigmoidal dynamics explains the data much better than Olson's model.

We must stress the fact that, according to such a dynamics, r continuously increases with time. A decrease in the decomposition rate (due to the accumulation of recalcitrant plant polymers and/or residual by-products of microbial activity, such as humic substances) is not yet detectable. If such a phenomenon occurs, it will only do so in

Table 4

Dataset C (Berg et al., 2003). Parameters for the best-fitting to Eq. (21), which was the originally applied by Berg et al. to study their data.

Site	Species	<i>k</i>	<i>m</i>	R^2
Jädraås	Green <i>Populus tremula</i>	0.230	62.74	0.910
	Brown <i>Populus tremula</i>	0.214	63.00	0.940
	Green <i>Pinus sylvestris</i>	0.160	72.76	0.949
	Brown <i>Pinus sylvestris</i>	0.091	82.86	0.958
	<i>Pinus contorta</i>	0.062	100.00	0.933
	<i>Betula pubescens</i>	0.200	62.28	0.933
	<i>Pinus pinea</i>	0.081	77.76	0.940
Monte Taburno	Green <i>Populus tremula</i>	0.224	79.71	0.965
	Brown <i>Populus tremula</i>	0.208	77.63	0.975
	Green <i>Pinus sylvestris</i>	0.130	85.05	0.994
	Brown <i>Pinus sylvestris</i>	0.165	74.34	0.994
	<i>Pinus contorta</i>	0.084	100.00	0.941
	<i>Betula pubescens</i>	0.325	69.56	0.988
	<i>Pinus pinea</i>	0.110	67.76	0.992

the very long term, beyond the time scope of this dataset, and will obviously affect a very small fraction of the initial litter.

We did not detect significant statistical relationships between any of the parameters of the fitting curves and the initial biochemical characteristics of the studied litters (not shown). Most of the litter disappeared in less than 1 year in all cases: such an intense decomposition may indicate that litter quality was not a relevant constraint at any stage. It is also possible that the true constraints for litter decomposition were not the parameters analysed by the authors (content of hemicellulose and cellulose, lignin), but rather alternatives not included in this study: for instance, Mn content (Berg et al., 2007), or physical properties of leaves such as toughness (Gallardo and Merino, 1993; Pérez-Harguindeguy et al., 2000).

3.5. Dataset E (Li et al., 2007)

The data of Li et al. (2007) are summarised in Fig. 11, together with the curves that match best. For all litters, the decomposition data matched well with a rational-type dynamics, assuming $d = 3$ (Eq. (20), placed in Eq. (8)). Fig. 12 shows the dynamics of decomposition, as obtained from Eq. (15); the fitted values for the several parameters are summarised in Table 6. The degree of the fit was always > 0.96 , higher than that obtained with Olson's equation (Table A1). It is often found that $c = 0$; when this was not the case, c was always very low. Therefore we repeated the curve fitting, suppressing c from the Eq. (20), thus reducing the number of parameters to be fitted down to only two. The new R^2 values were

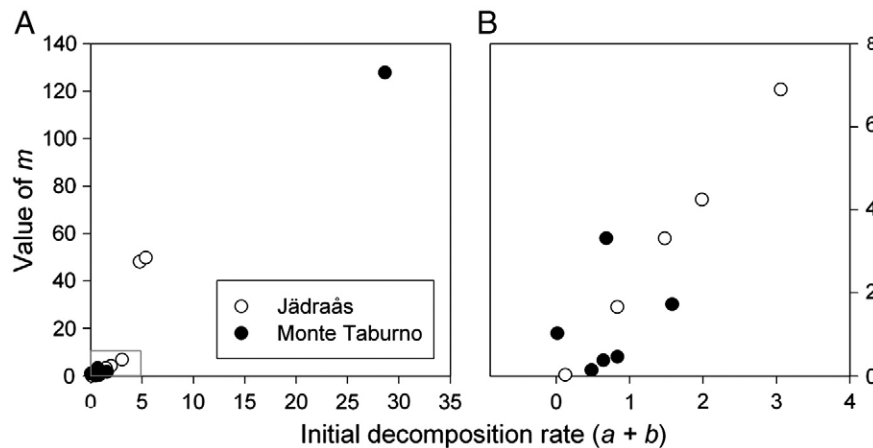


Fig. 9. Dataset C: relationship between the initial decomposition rate ($a + b$) and its decay (m). A: all data. B: detail of panel A, for the smallest $a + b$ values (small square, within panel A).

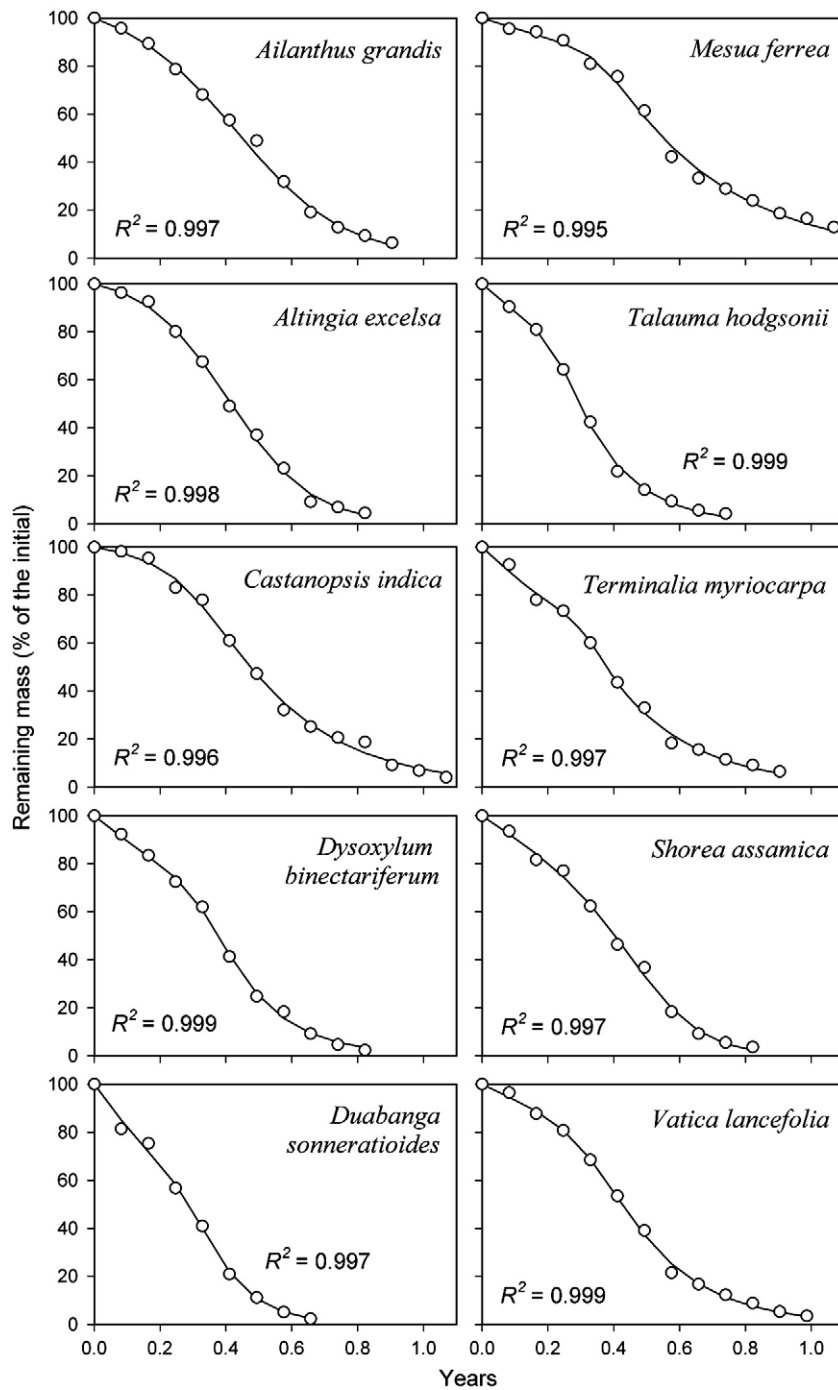


Fig. 10. Results obtained for dataset D. Experimental data have been fitted to a positive-sigmoidal curve (Eq. (14), placed in Eq. (8)). Parameters are given in Table 5.

Table 5

Dataset D (Rahman Barbhuiya et al., 2008). Parameters of the best-fitting sigmoidal curves obtained (Eq. (14), placed in Eq. (8)). The obtained curves and R^2 values are shown in Fig. 10.

Species	a	b	c	t_0
<i>Ailanthus grandis</i>	6.5597	-0.1446	0.4422	0.5086
<i>Mesua ferrea</i>	2.4427	-0.0388	0.4377	0.3650
<i>Altingia excelsa</i>	8.2227	-0.1295	0.0000	0.4173
<i>Talauma hodgsonii</i>	5.1669	-0.0292	1.2092	0.2341
<i>Castanopsis indica</i>	3.5107	-0.0777	0.1827	0.3079
<i>Terminalia myriocarpa</i>	2.8247	-0.0156	1.3028	0.3047
<i>Dysoxylum binectariferum</i>	5.1169	-0.0435	1.1140	0.3379
<i>Shorea assamica</i>	9.3008	-0.1096	0.8217	0.4933
<i>Duabanga sonneratioides</i>	6.9681	-0.0413	1.9632	0.3109
<i>Vatica lanceifolia</i>	4.3121	-0.0659	0.6297	0.3437

identical to the previous ones; therefore these simplified models are those shown in Figs. 11 and 12, and also in Table A1.

To the eye, dataset E looks similar to dataset D (compare Figs. 10 and 11), but this similarity is only superficial. We tried to fit the data of Li et al. (2007) to Eq. (14) (placed in Eq. (8)), i.e., to assume a positive-sigmoidal dynamics for the decomposition rate, but the results were not satisfactory (data not shown). Thus, for dataset E it was necessary to assume that, after a period of increase, r finally decreases in all litters, in contrast with the results obtained with dataset D, in which r increased continuously in all litters. In addition to differences in litter quality, the differences in climate (tropical in dataset D, cold monsoonic in dataset E) may be responsible for these contrasting evolutions.

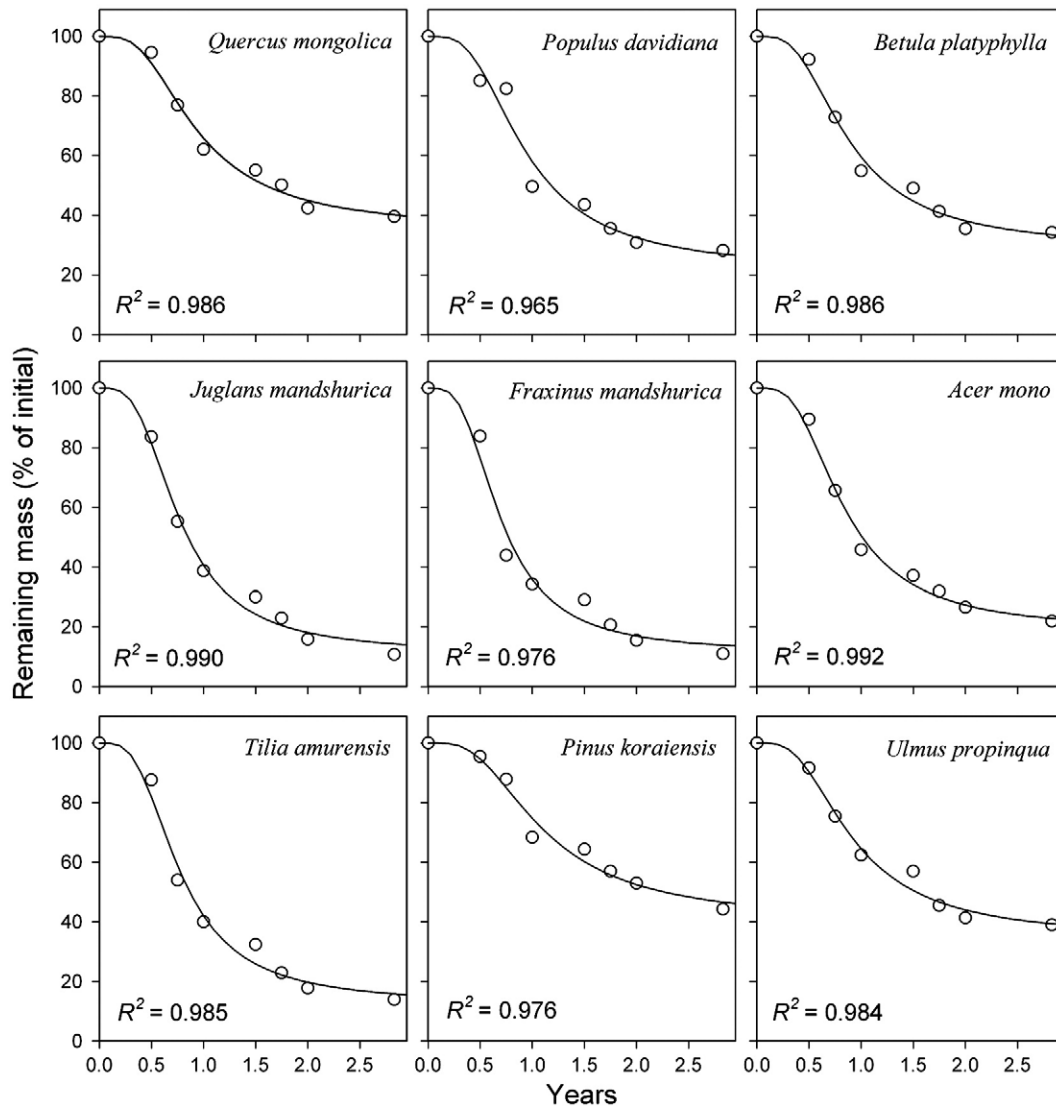


Fig. 11. Results obtained for dataset E. Experimental data have been fitted to a rational-type curve (Eq. (20), placed in Eq. (8)). Parameters are given in Table 6.

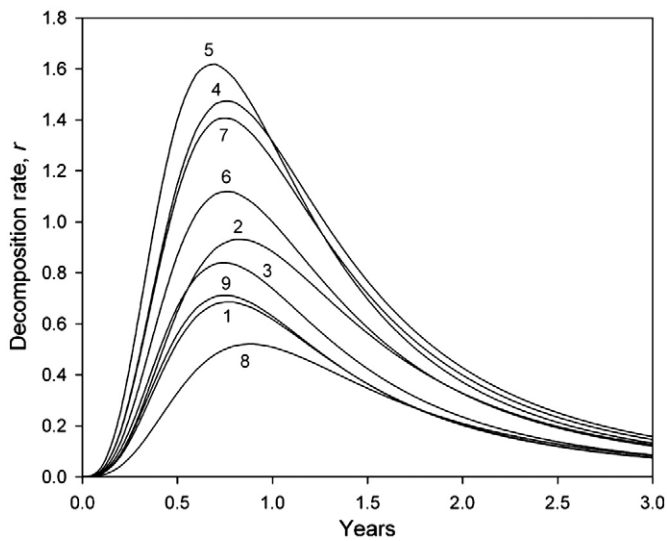


Fig. 12. Changes in the decomposition rates for the several litters of dataset E, as given by applying to Eq. (15) the parameters given in Table 6. 1: *Quercus mongolica*. 2: *Populus davidiana*. 3: *Betula papyrifera*. 4: *Juglans mandshurica*. 5: *Fraxinus mandshurica*. 6: *Acer mono*. 7: *Tilia amurensis*. 8: *Pinus koraiensis*. 9: *Ulmus propinqua*.

Table 6

Dataset E (Li et al., 2007). Results for curve fitting: values obtained for the three parameters. Decomposition data have been fitted to rational-type dynamics, assuming $d = 3$ (Eq. (20), placed in Eq. (8)). (a) Original results for the three parameters: a , b , c . (b) Repetition of the fitting for the four species in which originally $c > 0$, but deleting c in the equation. The obtained curves are shown in Fig. 11, together with the obtained R^2 values.

Species	a	b	c
a) Original results			
<i>Quercus mongolica</i>	1.3514	0.5868	0.0000
<i>Populus davidiana</i>	1.6135	0.6836	0.0020
<i>Betula platyphylla</i>	1.4041	0.5535	0.0000
<i>Juglans mandshurica</i>	1.7054	0.5826	0.0446
<i>Fraxinus mandshurica</i>	1.6060	0.4675	0.0000
<i>Acer mono</i>	1.5749	0.5750	0.0000
<i>Tilia amurensis</i>	1.6782	0.5603	0.0000
<i>Pinus koraiensis</i>	1.3908	0.7929	0.0252
<i>Ulmus propinqua</i>	1.3132	0.5640	0.0242
b) Repetition, deleting c			
<i>Populus davidiana</i>	1.6147	0.6828	–
<i>Juglans mandshurica</i>	1.7229	0.5725	–
<i>Pinus koraiensis</i>	1.4182	0.7768	–
<i>Ulmus propinqua</i>	1.3388	0.5619	–

4. Discussion

4.1. Precedents of our approach

Throughout the past century, to fit decomposition datasets some authors suggested equations which were based on the two assumptions which also form the basis of our study: (i) the decomposing organic matter is taken as a unique pool, avoiding switching it into labile and recalcitrant compartments, and (ii) for this unique compartment, a non-constant decomposition rate is assumed. These studies are clear precedents of our approach, and important to mention.

Thus, Godshalk and Wetzel (1978) suggested a variation in Olson's equation in which the instantaneous decomposition rate decayed exponentially with time. Such an approach is a clear precedent of Case 1 studied in this paper. The main difference is that in Godshalk and Wetzel's approach the asymptotical end value of the decomposition rate is necessarily 0, in contrast with our approach (Eq. (9)). Almost a decade later, Ezcurra and Becerra (1987) studied several datasets of litter decomposition in tropical forests, and suggested replacing the constant term k in Eq. (4) by several functions, i.e., to repeat the process given by Olson (1963) but assuming a non-constant decomposition rate.

In all of these precedents, the decomposition rate was assumed to decrease with time. We did not make this assumption: in our approach, r may follow virtually any behaviour. The only limitation is that this behaviour must make biological sense.

4.2. Main features: discussion

Our approach allows to fit virtually any decomposition dataset, as long as (i) the change in the decomposition rate can be described as a mathematical equation, and (ii) this equation is integrable in the interval $(0, t)$, where t is the total decomposition time. This second condition can be a problem. If the function is not integrable, then the integral could be approached by numerical methods, but this implies that the decomposition data cannot be fitted directly, by algorithms such as that of Marquardt–Levenberg, to obtain the parameters that fits best.

There could be as many models as datasets to fit, but in practice the ways in which r can change are finite. The examples we have shown can be applied to a wide range of experimental data. In the end, all the equations proposed in this paper deal with three basic questions: (i) what is the initial r , (ii) what is the final r , and (iii) how the change in r occurs. The third point (iii) determines the kind of equation chosen for the behaviour of r . All the equations shown in this paper may be interpreted in biological terms, and their application yields results that suggest future research. Thus, it is worth looking in more detail at the apparent lack of decrease in litter quality in dataset B, even following the loss of over 50% of the litter (the rhythmic fluctuations in r , likely seasonal, are enough to explain this data). It is also worth studying the increase in litter quality in dataset D (as deduced from the application of a positive-sigmoidal dynamic for r), by studying the biochemical changes occurring in the decomposed litters.

The first handicap of our approach is that the number of parameters needed for the proposed curves is relatively high (3 or more). Unfortunately, this is almost unavoidable. If the changes in the decomposition rate (r) must be reflected in a mathematical way, at least three parameters are needed: two to state the uppermost and the lowermost possible values for r , and also parameters (1, at least) that in the equation we apply will determine the shape of the change and/or how fast the change occurs. The models may be simplified: for instance, the rational model (3 parameters, assuming $d = 3$) becomes a 2-parameter model if we suppress the constant term (c) from Eq. (20). Simplifications, however, should be done *a posteriori*, only if one of the parameters is found to be really unnecessary, which will

not always occur. This can be a problem when applying strict statistical criterions (e.g., Akaike's) to establish whether the new equation may be preferred to a simpler one (e.g., Olson's), because the decomposition datasets are often small (less than 10 points, for instance), and AIC strongly penalizes complex equations, even when the fit is greatly improved. The dataset of *V. vitis-idaea* (Table A1: dataset A) is an example of this: the composite-exponential equation fits the data clearly better than the Olson's, but the increase in both AIC and AIC_c is negative, owing clearly to the small dataset (only 6 points). The results given in Table A1 stress that, for a given decomposition experiment, establishing the kind of dynamics (e.g., single-exponential, composite-exponential, sigmoidal, etc.) may be impossible if the dataset is too small.

A second drawback of our approach is that the integrated equations cannot always be simple. The composite-exponential equation (Eq. (9)) has quite a simple integrated form (Eq. (10)), but the rest of the integrated forms are much more complex than the conventional—and most widely used—double-exponential equation (Eq. (3)). Nevertheless, this should not be a serious obstacle to applying our approach, since most of the current statistical packages include powerful and user-friendly tools for curve fitting, which allow the fit of complex equations in a very short time. The need to solve the integral of $f(t)$ can be seen as a serious handicap; nevertheless, the availability of mathematical compilations of solved integral equations (Abramowitz and Stegun, 2008), showing the solution of a very high number of useful formulas, is a helpful option for researchers who are not used to standard calculus.

Researchers should be careful when choosing an equation to fit decomposition data. The simplicity of the equation is often the main criterion for choosing it, because many authors look for an easy way to compare many datasets (many different species in the same paper, for instance). The availability of computer tools for curve fitting makes it a merely routine practice, which is risky when the chosen equation (often, the Olson's equation) does not properly match the experimental data. A different problem also arises when the equation chosen gives a good fit, but describes a process that does not agree with what happens in nature. The double-exponential model (Eq. (3)) is a good example of this. The results obtained with dataset A (Fig. 5, Table 1) stress that contrasted equations can give very similar, if not almost identical curves, at least within the range of the experimental data. Conversely, the good fit obtained when applying a given equation does not imply that this equation truly reflects what happens in the decomposition process. In contrast with the double-exponential model (Eq. (3)), none of the equations we propose in this paper makes any *a priori* hypothesis about the internal structure of the decomposing substrate (i.e., its split into functional compartments), a fact that may look unfair for some researchers, but that gives a high robustness to our approach.

5. Conclusions

We propose a generalised exponential approach to the decomposition process, more flexible than others currently available, for it considers the possibility of increases, decreases, and rhythmical changes in the decomposition rate. Thanks to this approach, it is possible to obtain equations that match a wide number of decomposition datasets, equations of which we give several examples. In all cases, the parameters of the proposed equations have a clear meaning, as they affect the shape of the obtained curve. Thus, for many datasets the application of our approach allows an interpretation of their results in biological terms.

Acknowledgements

The work of one of the authors (Pere Rovira) is partly funded by the Spanish Ministry of Science and Innovation, through the research

CONSOLIDER programme (GRACCIE net). We also would like to thank Mr. Björn Berg, who kindly gave us the numerical data for a great number of decomposition experiments, and Catherine Amette for her review of our English text. The advice given by Fernando Maestre on the application of Akaike's concept is also greatly acknowledged.

Appendix A

Table A1

Results of fitting the single-exponential model (Olson's equation: Eq. (1)) to all datasets. The R^2 obtained by applying the proposed equations is given also for a direct comparison. The increase in AIC and AIC_C is given.

Species	Single-exponential		Proposed ^a		Akaike criterion	
	k	R ²	R ²	Δ AIC	Δ AIC _C	
i) Dataset A (Berg et al., 1984)						
<i>Pinus sylvestris</i>	0.2977	0.984	0.993	2.455	4.330	
<i>Betula pubescens</i>	0.3522	0.763	0.990	-10.818	-7.834	
<i>Vaccinium vitis-idaea</i>	0.2576	0.874	0.985	-1.200	9.800	
ii) Dataset B (Berg et al., 1984)						
<i>Pinus strobus</i>	0.3436	0.916	0.997	-10.276	-4.054	
<i>Quercus alba</i>	0.4164	0.926	0.996	-4.263	1.959	
<i>Quercus borealis</i>	0.3862	0.943	0.993	-3.341	2.881	
iii) Dataset C (Berg et al., 2003). Data from Jädraås						
<i>Pinus sylvestris</i> green	0.4246	0.852	0.964	-2.396	0.204	
<i>Pinus sylvestris</i> brown	0.3006	0.930	0.975	0.663	3.263	
<i>Pinus pinea</i>	0.2536	0.894	0.969	-0.084	2.516	
<i>Pinus contorta</i>	0.2069	0.957	0.932	-2.245	0.356	
<i>Populus tremula</i> green	0.4350	0.519	0.976	-10.355	-7.755	
<i>Betula pubescens</i>	0.4070	0.529	0.978	-9.709	-7.109	
<i>Populus tremula</i> brown	0.4192	0.605	0.990	-14.830	-12.230	
iv) Dataset C (Berg et al., 2003). Data from Monte Taburno						
<i>Pinus sylvestris</i> green	0.4808	0.981	0.994	1.231	4.215	
<i>Pinus sylvestris</i> brown	0.4344	0.987	0.993	-3.286	-0.301	
<i>Pinus pinea</i>	0.3364	0.964	0.997	-7.788	-4.804	
<i>Pinus contorta</i>	0.2958	0.953	0.941	-6.451	-3.467	
<i>Populus tremula</i> green	0.6594	0.923	0.984	-3.369	-0.385	
<i>Betula pubescens</i>	0.6221	0.886	0.994	-12.843	-9.859	
<i>Populus tremula</i> brown	0.6007	0.960	0.973	-0.428	2.556	
v) Dataset D (Rahman Barbhuiya et al., 2008)						
<i>Ailanthus grandis</i>	1.7988	0.887	0.997	-10.620	-4.398	
<i>Mesua ferrea</i>	1.3488	0.872	0.995	-12.553	-7.916	
<i>Altingia excelsa</i>	1.9995	0.856	0.998	-12.713	-5.213	
<i>Talauma hodgsonii</i>	2.8764	0.911	0.999	-12.021	-2.593	
<i>Castanopsis indica</i>	1.6844	0.883	0.996	-13.036	-8.400	
<i>Terminalia myriocarpa</i>	2.1951	0.934	0.997	-9.106	-2.884	
<i>Dysoxylum binectariferum</i>	2.3230	0.895	0.999	-13.353	-5.853	
<i>Shorea assamica</i>	2.1649	0.887	0.997	-10.116	-2.616	
<i>Duabanga sonneratioides</i>	3.1513	0.926	0.997	-5.396	7.271	
<i>Vatica lancefolia</i>	1.9902	0.891	0.999	-15.758	-10.444	
vi) Dataset E (Li et al. 2007)						
<i>Quercus mongolica</i>	0.3794	0.937	0.986	-2.602	-0.402	
<i>Populus davidiana</i>	0.5198	0.917	0.965	-0.595	1.605	
<i>Betula platyphylla</i>	0.4621	0.930	0.986	-2.964	-0.764	
<i>Juglans mandshurica</i>	0.7961	0.954	0.990	-2.684	-0.484	
<i>Fraxinus mandshurica</i>	0.8704	0.932	0.976	-1.111	1.089	
<i>Acer mono</i>	0.6138	0.940	0.992	-3.972	-1.772	
<i>Tilia amurensis</i>	0.7613	0.937	0.985	-2.268	-0.068	
<i>Pinus koraiensis</i>	0.2956	0.935	0.976	-0.951	1.249	
<i>Ulmus propinqua</i>	0.3934	0.947	0.985	-1.733	0.467	

^a Composite-exponential (datasets A and C), sinusoidal (dataset B), sigmoidal (dataset D), rational (dataset E).

Appendix B. Obtaining the integrated forms of the studied equations

The general form is:

$$X_t = X_0 e^{-\left(\int_0^t f(t) dt\right)} \tag{8}$$

and therefore the problem to solve is to integrate $f(t)$, for the several functions we can imagine. Here we describe the obtention of the integrated forms of the four examples of $f(t)$ suggested in this paper.

Case 1. Exponential decay of the decomposition rate.

$$f(t) = a + be^{-mt} \tag{A1}$$

We integrate Eq. (A1):

$$\int_0^t (a + be^{-mt}) dt = \left[at + \frac{be^{-mt}}{m} \right]_0^t \tag{A2}$$

$$\left[at + \frac{be^{-mt}}{m} \right]_0^t = at - \frac{be^{-mt}}{m} + \frac{b}{m} = at - \frac{b}{m} (e^{-mt} - 1) \tag{A3}$$

Case 2. Wave-form changes in the decomposition rate.

The function that describes the changes in the decomposition rate r is

$$f(t) = m + a \sin\left(\frac{2\pi}{b}t + c\right) \tag{A4}$$

where a, b, c and m are constants. The integral of such a function, as in most of trigonometric integrals, is almost immediate:

$$\int_0^t f(t) dt = \int_0^t \left[m + a \sin\left(\frac{2\pi}{b}t + c\right) \right] dt = \tag{A5}$$

$$= mt + \frac{ab}{2\pi} \int_0^t \frac{2\pi}{b} \sin\left(\frac{2\pi}{b}t + c\right) dt = \left[mt - \frac{ab}{2\pi} \cos\left(\frac{2\pi}{b}t + c\right) \right]_0^t = \tag{A6}$$

$$m(t-0) - \frac{ab}{2\pi} \left[\cos\left(\frac{2\pi}{b}t + c\right) - \cos c \right] \tag{A7}$$

From Eq. (A7), Eq. (12) is obtained immediately.

Case 3. Sigmoidal decrease or increase of the decomposition rate.

The function that describes the changes in the decomposition rate r is

$$f(t) = \frac{a}{1 + e^{\frac{t-t_0}{b}}} + c \tag{A8}$$

So the integral is:

$$\int_0^t f(t) dt = ct + \int_0^t \frac{a}{1 + e^{\frac{t-t_0}{b}}} dt \tag{A9}$$

To solve the second term, a change of variable has been applied:

$$x = \frac{t-t_0}{b} \rightarrow bdx = dt \tag{A10}$$

Then, it becomes

$$\int_0^t \frac{a}{1 + e^{\frac{t-t_0}{b}}} dt = ab \int_{-\frac{t_0}{b}}^{\frac{t-t_0}{b}} \frac{1}{1 + e^x} dx \tag{A11}$$

This integral can be easily obtained using the following equation (Spiegel, 1970; equation 14.515, adapted):

$$\int \frac{1}{1 + e^x} dx = x - \ln(1 + e^x) \tag{A12}$$

Therefore:

$$\int_0^t \frac{a}{1 + e^{-t/b}} dt = ab \int_{-t_0/b}^{t-t_0/b} \frac{1}{1 + e^x} dx = ab[x - \ln(1 + e^x)]_{-t_0/b}^{t-t_0/b} \tag{A13}$$

And, finally,

$$\begin{aligned} &= ab \left[\frac{t-t_0}{b} - \ln\left(1 + e^{\frac{t-t_0}{b}}\right) + \frac{t_0}{b} + \ln\left(1 + e^{-\frac{t_0}{b}}\right) \right] \\ &= a \left[t - b \ln \frac{1 + e^{-\frac{t_0}{b}}}{1 + e^{-\frac{t-t_0}{b}}} \right] \end{aligned} \tag{A14}$$

We finally re-build the overall equation:

$$\int_0^t f(t) dt = ct + a \left[t - b \ln \frac{1 + e^{-(t_0-t)/b}}{1 + e^{-t_0/b}} \right] \tag{A15}$$

which is Eq. (14) of this paper.

Case 4. Rational-type change of the decomposition rate.

The equation that describes the changes in the decomposition rate *r* is

$$f(t) = c + \left(\frac{at}{t^2 + b} \right)^d \tag{A16}$$

Whatever the value of *d*, the integral can be decomposed in the following way:

$$\int_0^t f(t) dt = \int_0^t c dt + \int_0^t \left(\frac{at}{t^2 + b} \right)^d dt = ct + \int_0^t \left(\frac{at}{t^2 + b} \right)^d dt \tag{A17}$$

and hence the problem becomes simplified to solve the second component of the right term of the equation. There is no general solution for this equation, but a particular solution for each possible value of *d*.

For *d*=1, the solution is rather immediate (logarythm of the denominator). Hence we can write

$$\int_0^t f(t) dt = ct + \frac{a}{2} [\ln(t^2 + b)]_0^t = ct + \frac{a}{2} \ln\left(\frac{t^2 + b}{b}\right) \tag{A18}$$

For *d*>1 the solution is less simple. To obtain the integral form, a change of variable has been applied:

$$t = z\sqrt{b} \tag{A19}$$

and thus the integral form of Eq. (A17) becomes

$$\int_0^t \left(\frac{at}{t^2 + b} \right)^d dt = \frac{a^d}{\sqrt{b^{d-1}}} \int_0^{t/\sqrt{b}} \frac{z^d}{(z^2 + 1)^d} dz \tag{A20}$$

We re-write the subintegral part of Eq. (A20) in a different form:

$$\frac{z^d}{(z^2 + 1)^d} = z^{d-1} \frac{z}{(z^2 + 1)^d} \tag{A21}$$

and we replace Eq. (A21) in Eq. (A20). Then, we integrate by steps:

$$\frac{a^d}{\sqrt{b^{d-1}}} \int_0^{t/\sqrt{b}} \frac{z^d}{(z^2 + 1)^d} dz = \frac{a^d}{\sqrt{b^{d-1}}} \int_0^{t/\sqrt{b}} z^{d-1} \frac{z}{(z^2 + 1)^d} dz \tag{A22}$$

Let us take:

$$dv = \frac{z}{(z^2 + 1)^d} dz \rightarrow v = \frac{1}{(2-2d)(z^2 + 1)^{d-1}} \tag{A23}$$

$$u = z^{d-1} \rightarrow du = (d-1)z^{d-2} dz \tag{A24}$$

Then applying the well-known integration by steps formula:

$$\int_a^b uv dv = [uv]_a^b - \int_a^b v du \tag{A25}$$

we obtain:

$$\begin{aligned} &\frac{a^d}{\sqrt{b^{d-1}}} \int_0^{t/\sqrt{b}} z^{d-1} \frac{z}{(z^2 + 1)^d} dz = \\ &= \frac{a^d}{\sqrt{b^{d-1}}} \left\{ \frac{1}{2-2d} \left[\left(\frac{z}{z^2 + 1} \right)^{d-1} \right]_0^{t/\sqrt{b}} - \frac{d-1}{2-2d} \int_0^{t/\sqrt{b}} \frac{z^{d-2}}{(z^2 + 1)^{d-1}} dz \right\} \end{aligned} \tag{A26}$$

We re-write a bit the above equation:

$$\begin{aligned} &\int_0^t \left(\frac{at}{t^2 + b} \right)^d dt \\ &= \frac{a^d}{\sqrt{b^{d-1}}} \left\{ \frac{1}{2-2d} \left[\left(\frac{z}{z^2 + 1} \right)^{d-1} \right]_0^{t/\sqrt{b}} + \frac{1}{2} \int_0^{t/\sqrt{b}} \frac{z^{d-2}}{(z^2 + 1)^{d-1}} dz \right\} \end{aligned} \tag{A27}$$

and, adding the constant term (*ct*), the general solution for *d*>1 is

$$\begin{aligned} &\int_0^t c + \left(\frac{at}{t^2 + b} \right)^d dt \\ &= ct + \frac{a^d}{\sqrt{b^{d-1}}} \left\{ \frac{1}{2-2d} \left[\left(\frac{z}{z^2 + 1} \right)^{d-1} \right]_0^{t/\sqrt{b}} + \frac{1}{2} \int_0^{t/\sqrt{b}} \frac{z^{d-2}}{(z^2 + 1)^{d-1}} dz \right\} \end{aligned} \tag{A28}$$

which is Eq. (18) of this paper.

We must mention that, for *d*>1, an alternative way to solve Eq. (A17) would be through an iterative procedure. The primitive function may be obtained by applying the following recurrent development (Spiegel, 1970; equation 14.142):

$$\int \frac{x^m}{(x^2 + a^2)^n} dx = \int \frac{x^{m-2}}{(x^2 + a^2)^{n-1}} dx - a^2 \int \frac{x^{m-2}}{(x^2 + a^2)^n} dx \tag{A29}$$

By applying this approach to our problem (i.e., replacing *x* by *t*, and *n* by *d*), we finally obtain for *d*=2 and *d*=3 the same results (i.e., Eqs. (19) and (20)), even though the procedure is much longer than that proposed in this appendix. For *d*>3, the application of Eq. (A29) to our problem gives highly complex, poorly useful mathematical equations, not shown here.

References

- Abramowitz, M., Stegun, I., 2008. Handbook of mathematical functions with formulas, graphs, and mathematical tables, First paper edition. National Institute of Standards and Technology. electronic version freely available: <http://www.math.sfu.ca/~cbm/aands/>.
- Adair, E.C., Parton, W.J., Del Grosso, S.J., Silver, W.L., Harmon, M.E., Hall, S.A., Burke, I.C., Hart, S.C., 2008. Simple three-pool model accurately describes patterns of long-term litter decomposition in diverse climates. *Global Change Biology* 14, 2636–2660.
- Anderson, D.R., 2008. Model Based Inference in the Life Sciences. A Primer on Evidence. Springer, New York, USA.
- Berg, B., Laskowski, R., 2006. Litter Decomposition: A Guide to Carbon and Nutrient Turnover. Academic Press, USA. 421 pp.
- Berg, B., Hannus, K., Popoff, Th., Theander, O., 1982. Changes in organic chemical components of needle litter during decomposition. Long-term decomposition in a Scots pine forest, I. *Canadian Journal of Botany* 60, 1310–1319.
- Berg, B., Ekbohm, G., McLaugherty, C., 1984. Lignin and holocellulose relations during long-term decomposition of some forest litters long-term decomposition in a Scots pine forest. IV. *Canadian Journal of Botany* 62, 2540–2550.
- Berg, B., Ekbohm, G., Johansson, M., McLaugherty, C., Rutigliano, F., Virzo De Santo, A., 1996. Maximum decomposition limits of forest litter types: a synthesis. *Canadian Journal of Botany* 74, 659–672.
- Berg, B., Virzo De Santo, A., Rutigliano, F.A., Fierro, A., Ekbohm, G., 2003. Limit values for plant litter decomposing in two contrasting soils Influence of litter elemental composition. *Acta Oecologica* 24, 295–302.
- Berg, B., Steffen, K.T., McLaugherty, C., 2007. Litter decomposition rate is dependent on litter Mn concentrations. *Biogeochemistry* 82, 29–39.
- Bosatta, E., Ågren, G.I., 1985. Theoretical analysis of decomposition of heterogeneous substrates. *Soil Biology & Biochemistry* 17, 601–610.
- Bosatta, E., Ågren, G.I., 1991. Dynamics of carbon and nitrogen in the organic matter of the soil. A generic theory. *The American Naturalist* 138, 227–245.
- Carpenter, S.R., 1981. Decay of heterogeneous detritus: a general model. *Journal of Theoretical Biology* 90, 539–547.
- Carpenter, S.R., 1982. Comparisons of equations for decay of leaf litter in tree-hole ecosystems. *Oikos* 39, 17–22.
- Coûteaux, M.M., Bottner, P., Anderson, J.M., Berg, B., Bolger, T., Casals, P., Romanyà, J., Thiéry, J.M., Vallejo, V.R., 2001. Decomposition of ¹³C-labelled standard plant material in a latitudinal transect of European coniferous forests: differential impact of climate on the decomposition of soil organic matter compartments. *Biogeochemistry* 54, 147–170.
- Dendooven, L., Merckx, R., Verstraeten, L.M.J., Vlassak, K., 1997. Failure of an iterative curve-fitting procedure to successfully estimate two organic N pools. *Plant and Soil* 195, 121–128.
- Ezcurra, E., Becerra, J., 1987. Experimental decomposition of litter from the Tamaulipan cloud forest. A comparison of four simple models. *Biotropica* 19, 290–296.
- Feng, Y., 2009a. Fundamental considerations of soil organic carbon dynamics: a new theoretical framework. *Soil Science* 174, 467–481.
- Feng, Y., 2009b. K-model—a continuous model of soil organic carbon dynamics: theory. *Soil Science* 174, 482–493.
- Feng, Y., 2009c. K-model—A continuous model of soil organic carbon dynamics: model parametrization and testing. *Soil Science* 174, 494–507.
- Gallardo, A., Merino, J., 1993. Leaf decomposition in 2 Mediterranean ecosystems of Southwest Spain—Influence of substrate quality. *Ecology* 74, 152–161.
- Gillon, D., Joffre, R., Ibrahima, A., 1993. Initial litter properties and decay rate: a microcosm experiment on Mediterranean species. *Canadian Journal of Botany* 72, 946–954.
- Godshalk, G.L., Wetzel, R.G., 1978. Decomposition of aquatic angiosperms II. Particulate components. *Aquatic Botany* 5, 301–327.
- Jenny, H., Gessel, S.P., Bingham, F.T., 1949. Comparative study of decomposition rates of organic matter in temperate and tropical regions. *Soil Science* 68, 419–432.
- Kelley, K.R., Stevenson, F.J., 1996. Organic forms of N in soil. In: Piccolo, A. (Ed.), *Humic Substances in Terrestrial Ecosystems*. Elsevier, Amsterdam, pp. 407–427.
- Li, X., Han, S., Zhang, Y., 2007. Foliar decomposition in a broadleaf-mixed Korean pine (*Pinus koraiensis* Sieb. et Zucc.) plantation forest: the impact of initial litter quality and the decomposition of three kinds of organic matter fraction on mass loss and nutrient release rates. *Plant and Soil* 295, 151–167.
- Lousier, J.D., Parkinson, D., 1976. Litter decomposition in a cool temperate deciduous forest. *Canadian Journal of Botany* 54, 419–436.
- Minderman, G., 1968. Addition, decomposition and accumulation of organic matter in forests. *Journal of Ecology* 56, 355–362.
- Montaña, C., Ezcurra, E., Carrillo, A., Delhoume, J.P., 1988. The decomposition of litter in grasslands of northern Mexico: a comparison between arid and non-arid environments. *Journal of Arid Environments* 13, 551–556.
- Nömmik, H., Vahtras, K., 1982. Retention and fixation of ammonium in soils. In: Dinauer, R.C. (Ed.), *Nitrogen in Agricultural Soils*. Agronomy Series, vol. 22. ASA-SSSA, Madison, USA, pp. 123–171.
- Olson, J.S., 1963. Energy storage and the balance of producers and decomposers in ecological systems. *Ecology* 44, 322–331.
- Pérez-Harguindeguy, N., Díaz, S., Cornelissen, J.H.C., Vendramini, F., Cabido, M., Castellanos, A., 2000. Chemistry and toughness predict leaf litter decomposition rates over a wide spectrum of functional types and taxa in central Argentina. *Plant and Soil* 218, 21–30.
- Rahman Barbhuiya, A., Arunachalam, A., Chandra Nath, P., Latif Khan, M., Arunachalam, K., 2008. Leaf litter decomposition of dominant tree species of Namdapha National Park, Arunachal Pradesh, northeast India. *Journal of Forest Research* 13 (25), 34.
- Rovira, P., Vallejo, V.R., 1997. Organic carbon and nitrogen mineralization under Mediterranean climatic conditions: the effects of incubation depth. *Soil Biology & Biochemistry* 29, 1509–1520.
- Rovira, P., Vallejo, V.R., 2000. Decomposition of *Medicago sativa* debris incubated at different depths under Mediterranean climate. *Arid Soil Research & Rehabilitation* 14, 265–280.
- Rovira, P., Vallejo, V.R., 2002. Labile and recalcitrant pools of carbon and nitrogen in organic matter decomposing at different depths in soil: an acid hydrolysis approach. *Geoderma* 107, 109–141.
- Rovira, P., Kurz-Besson, C., Coûteaux, M.M., Vallejo, V.R., 2008. Changes in litter properties during decomposition: a study by differential thermogravimetry and scanning calorimetry. *Soil Biology & Biochemistry* 40, 172–185.
- Spiegel, M., 1970. *Manual de fórmulas y tablas matemáticas*. McGraw-Hill, Mexico (Spanish translation of Schaum's Mathematical Handbook of Formulas and Tables, McGraw-Hill, USA, 1968).
- Vaieretti, M.V., Pérez Harguindeguy, N., Gurvich, D.E., Cingolani, A.M., Cabido, M., 2005. Decomposition dynamics and physico-chemical leaf quality of abundant species in a montane woodland in central Argentina. *Plant and Soil* 278, 223–234.
- Wieder, R.K., Lang, G.E., 1982. A critique of the analytical methods used in examining decomposition data obtained from litter bags. *Ecology* 63, 1636–1642.
- Wolters, V., Schaefer, M., 1993. Effects of burrowing by the earthworm *Aporrectodea caliginosa* (Savigny) on beech litter decomposition in an agricultural and in a forest soil. *Geoderma* 56, 627–632.
- Yang, H.S., Janssen, B.H., 2000. A mono-compartment model of carbon mineralization with a dynamic rate constant. *European Journal of Soil Science* 51, 517–529.
- Zhang, C.F., Meng, F.R., Bhatti, J.S., Trofymow, J.A., Arp, P.A., 2008. Modeling forest leaf-litter decomposition and N mineralization in litterbags, placed across Canada: a 5-model comparison. *Ecological Modelling* 219, 342–360.